# Resolution Capabilities of the DBIM-TwIST Algorithm in Microwave Imaging

Ziwen Guo, Syed Ahsan, Olympia Karadima, Ioannis Sotiriou, Panagiotis Kosmas
Department of Informatics, King's College London, London, UK, Email: panagiotis.kosmas@kcl.ac.uk

*Abstract*—We investigate resolution capabilities of adaptive thresholding methods in the context of iterative microwave imaging algorithms. Our test cases involve two closely located cylindrical targets of high dielectric contrast with respect to the background in a microwave tomography setup simulated in CST. We apply a distorted Born iterative method (DBIM), and compare a two-step iterative shrinkage thresholding (TwIST) implementation with a conventional conjugate gradient least squares (CGLS) method as linear solvers at each DBIM iteration. Our results demonstrate that applying the TwIST approach can resolve the two closely-located targets much more accurately than the CGLS under identical settings in the DBIM algorithm.

*Index Terms*—adaptive thresholding, DBIM, CGLS, TwIST, microwave imaging.

## I. INTRODUCTION

Microwave tomographic methods estimate the spatial distribution of dielectric properties in a reconstruction region by solving an electromagnetic (EM) inverse scattering problem [1]. The success of these methods depends on the deployed reconstruction algorithms as well as data quality acquired by the experimental setup [2]. Our previous work has shown good reconstruction results in a wideband microwave tomography system via the distorted Born iterative method (DBIM) [3]. The DBIM solves the nonlinear scattering problem iteratively by applying the Born approximation at each iteration and solving the resulting linear problem. The approach to this linear inverse problem is one of the most important factors for the overall convergence of the DBIM to accurate estimates of the true dielectric properties in the reconstruction region.

Our previous work has studied the impact of thresholding methods as linear solvers in DBIM reconstructions of anatomically complex numerical breast models [4]–[6]. This was done using data from simplified two-dimensional (2-D) microwave imaging simulations. This work, on the contrary, considers simple imaging scenarios of two targets in a homogeneous background, but uses data from accurate models of our experimental systems in CST's Microwave Studio simulations. By placing the two targets at close distance in various locations, we can assess the ability of our system to resolve them using the TwIST vs. the CGLS as linear solvers inside the DBIM iterations.

The remainder of the paper is organized as follows: Section II reviews our DBIM-TwIST algorithm, while Section III introduces the multi-target model and simulation setup. Section IV presents the reconstruction results based on the two different linear inversion strategies, which illustrates the advantages of DBIM-TwIST approach followed by a Conclusion section.

## II. METHODS

### A. Distorted Born Iterative Method (DBIM)

The DBIM can solve nonlinear EM inverse scattering problems iteratively to reconstruct the spatial distribution of dielectric properties within a region V [7]. It is based on a approximating the non-linear integral equation which describes the relationship of the electric field with the continuous spatial distribution of dielectric properties via the Born approximation,

$$E_s(r_n, r_m) = E(r_n, r_m) - E_b(r_n, r_m)$$
$$= \omega^2 \mu \int_V G_b(r_n, r) E_b(r, r_m)(\epsilon(r) - \epsilon_b(r) dr), \quad (1)$$

where $E$, $E_s$, $E_b$ denote total, scattered, and background fields, respectively, and $G_b$ is the dyadic Green's function for the background medium which can be estimated by $G_b = \frac{i}{\omega\mu} E_b$ [7]. The complex permittivity of the known background and unknown object are denoted as $\epsilon_b(r)$ and $\epsilon(r)$, respectively, and their difference is the contrast function $O(r)$.

### B. Two-Step Iterative Shrinkage Thresholding (TwIST)

The TwIST algorithm can be used to solve the linear problem at each DBIM iteration as a linear inverse problem (LIP) of estimating the unknown original image vector from the observation vector via the linear equation $Ax = y$. Many approaches to this LIP define a solution to be the minimizer of a convex objective function,

$$f(x) = \frac{1}{2}\|y - Ax\|_2^2 + \lambda\Phi(x) \quad (2)$$

where $\Phi$ is the regularization function and $\lambda$ is a weighting parameter.

Iterative thresholding algorithms have been proposed by many authors within different frameworks [8]–[10]. The TwIST is based on the algorithm in [11]. This algorithm presents a method of splitting the matrix to structure a two-step iterative equation:

$$x_{t+1} = (1-\alpha)x_{t-1} + (\alpha - \beta)x_t + \beta\Gamma_\lambda(x_t)$$
$$\Gamma_\lambda(x) = \Psi_\lambda(x + A^T(y - Ax)) \quad (3)$$

where $\alpha$ and $\beta$ are the parameters of the TwIST algorithm and $\Psi_\lambda$ is the denoising function which is based on the regularization function $\Phi$. The next estimate $x_{t+1}$ depends not only on
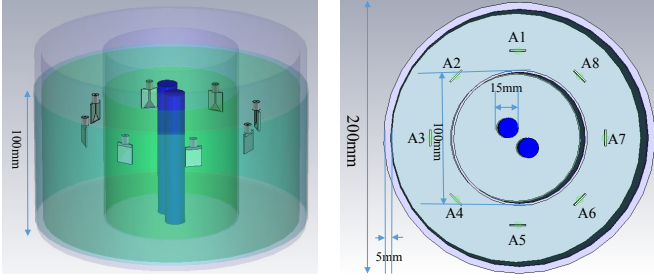
Fig. 1: Schematic of experimental setup modelled in CST Microwave Studio with eight antennas, the tank and targets.



Fig. 2: (a) Schematic of the proposed antenna modelled in CST Microwave Studio. (b) Photo of the fabricated antenna.

the current solution $x_t$, as in conventional iterative shrinkage thresholding algorithms, but also the previous solution $x_{t-1}$. In our previous work [5], we have studied the optimization of the parameters of the TwIST algorithm. The regularizer $\Phi(x)$ has been set as soft-thresholding function: $\Phi(x) = \|x\|_1$.

*C. Frequency-hopping*

Our recent work has demonstrated that the combination of multi-frequency information can enhance performance in terms of both robustness and resolution [6], [12]. In the frequency hopping approach, the single frequency reconstructions are performed from low to high frequencies [13]. Our experimental system can operate in the 1.0-3.0 GHz range [3]. The inverse problem involving higher contrasts can be solved better at lower frequencies due to the fact that the non-linear effect or multiple scattering effects are less pronounced at lower frequencies. Additionally, at lower frequencies the inverse problem converges using less number of iterations and as a result reduced computational time. Therefore, we used five frequencies in this range (1.2, 1.4, 1.6, 1.8 and 2.0 GHz) with a fixed number of 15 iterations for the first three frequencies and 20 iterations for 1.8 GHz and 2.0 GHz. For all reconstructions, cubic voxels of 2.0 mm side have been used in our imaging algorithm. At the start of the inversion process at 1.2 GHz, the imaging domain was filled with the background glycerine-water medium of known properties. The reconstructed properties at 1.2 GHz were then inserted as the initial guess for the reconstruction at 1.4 GHz, and so on.

## III. SIMULATION SETUP

Our microwave tomography system is based on an eight-element array comprised of compact and robust printed monopole antennas operating in 1.0-3.0 GHz when fully immersed in a 90% glycerol-water mixture. The system has been validated experimentally in our previous work [3], but in this paper we have modelled the system in CST Microwave Studio to benchmark performance in the absence of experimental errors.

Fig. 1 shows the schematic of the CST simulation setup which consists of two concentric cylindrical tanks with 100 and 200 mm diameter. Fig.2 (a) shows the front and rear views of the proposed printed monopole. The fabricated antenna is
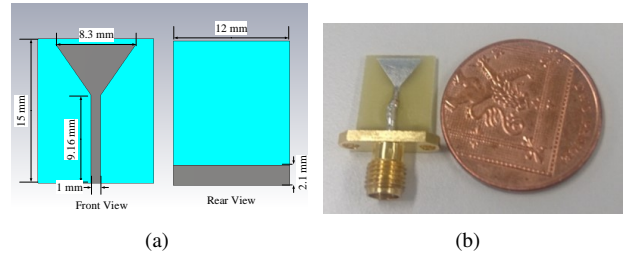
shown in Fig.2 (b). We have considered the antenna array diameter to be 130 mm, which helps maintaining the signal transmission levels above the noise floor. The targets are water-filled cylinders of 15 mm diameter placed inside the inner tank. Signals are recorded first in the homogeneous background and then with the dielectric cylindrical targets introduced. The simulation results from these cases produce the scattered signal information, which is used by the algorithm for reconstruction.

## IV. RECONSTRUCTION RESULTS

We present 2-D reconstruction results using the TwIST and CGLS solvers in conjunction with the DBIM. As in our previous work [3], all these reconstructions use the finite-difference time-domain (FDTD) method with a convolutional perfectly matched layer (CPML) boundary condition as forward solver in the DBIM. We also use a first-order Debye model to capture the dispersive behaviour of liquids such as the 90% glycerol-water mixture,

$$\epsilon_r(\omega) = \epsilon_\infty + \frac{\epsilon_s - \epsilon_\infty}{1 + j\omega\tau} - j\frac{\sigma_s}{\omega\epsilon_0} \tag{4}$$

where $\epsilon_\infty$, $\Delta\epsilon$, $\sigma_s$, and $\tau$ are the four parameters of the single-pole Debye model. We assume that the relaxation time constant $\tau$ is known and invariant with position, and reconstruct the Debye parameters which can then be used to calculate the resulting complex permittivity inside the reconstruction domain.

Fig.3 presents reconstructions of the targets depicted in Fig. 1 using the DBIM-TwIST and DBIM-CGLS algorithms. The actual real and imaginary permittivity values of the water targets at 1.2 GHz are $\epsilon'$=78.6 ,$\epsilon''$=4.8. For the DBIM-TwIST algorithm applied in the top row, both targets are detected and localised, and the estimated values are close to the actual, except for the imaginary part of the water target. For the CGLS algorithm applied in the bottom row, targets are not resolved well and appear as a single extended target, or with many artefacts around them.

To test further the ability of our algorithm to resolve close targets, we have considered additional CST models of varying targets distance. Fig.4 shows the top view of two CST simulation setups. The distances between the centres of the two targets in Fig.4 (a) and (b) are 40 and 20 mm, respectively. Fig.5 presents reconstructions of the permittivity's real part from the DBIM-TwIST and DBIM-CGLS algorithms for the
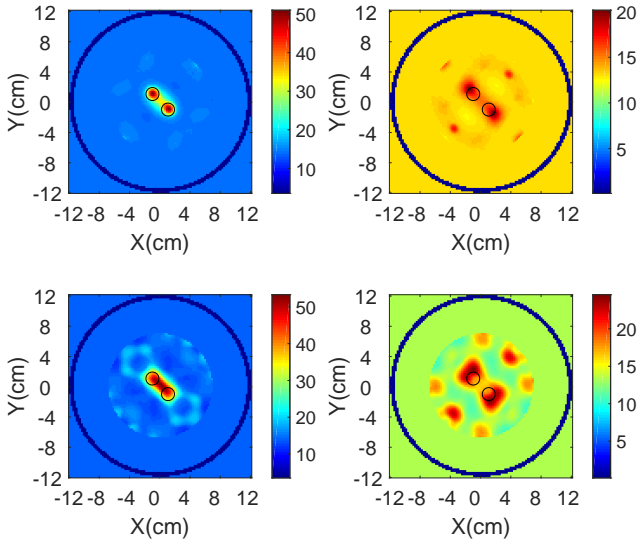
Fig. 3: Reconstructed real (left) and imaginary (right) part of the complex permittivity for the region inside the antenna array of Fig. 1. The top row corresponds to the TwIST algorithm, and the bottom row to CGLS. The complex permittivity was calculated at 1.2 GHz from the Debye parameters which were reconstructed using frequency hopping at 1.2, 1.4, 1.6, 1.8 and 2.0 GHz.
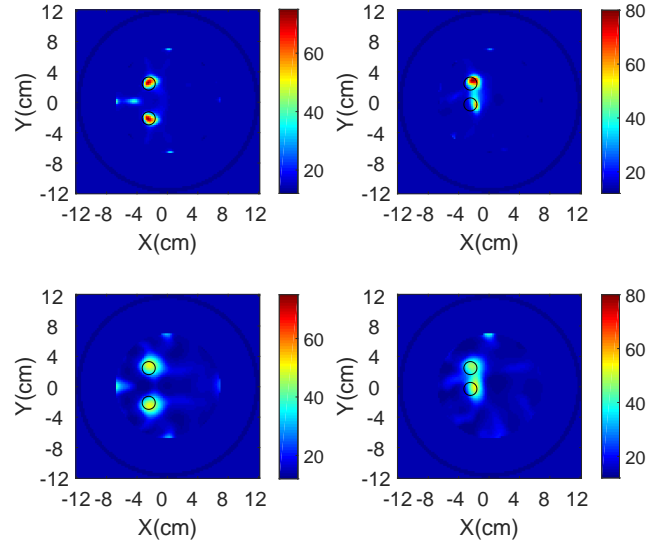


Fig. 5: Reconstructed real part of the complex permittivity for the CST setups of: (left) Fig. 4(a), and (right) Fig. 4(b). The top row corresponds to TwIST algorithm, and the bottom row to the CGLS. The complex permittivity was calculated at 1.2 GHz from the Debye parameters which were reconstructed using frequency hopping at 1.2, 1.4, 1.6, 1.8 and 2.0 GHz.
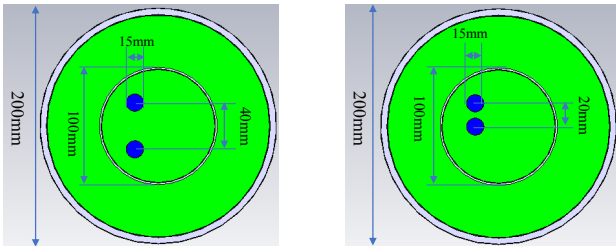


Fig. 4: Top view of two CST simulation models with varying target distance.

models of Fig.4. The top row corresponds to the TwIST algorithm, while the bottom row corresponds to the CGLS. It is again clear from these images that the TwIST outperforms the CGLS in resolving the two targets for these two different scenarios, and is also quantitatively more accurate in estimating the dielectric constant of the targets.

## V. Conclusion

We have considered 2-D microwave imaging scenarios based on CST simulation models of our experimental microwave tomography system to compare the TwIST and CGLS solvers in conjunction with the DBIM algorithm. The purpose of this study was to demonstrate that thresholding methods such as the TwIST can enhance resolution compared to traditional approaches such as the CGLS. Our results have shown

that the TwIST can resolve two closely located targets in in three different cases where the CGLS fails . A more extensive study including experimental results will be presented at the conference.

## References

[1] S. Semenov, "Microwave tomography: review of the progress towards clinical applications," *Philosophical Transactions of the Royal Society A: Mathematical, Physical and Engineering Sciences*, vol. 367, no. 1900, pp. 3021–3042, 2009.

[2] Z. Miao, S. Ahsan, and P. Kosmas, "Impact of information loss on reconstruction quality in microwave tomography for medical imaging," *Diagnostics*, vol. 8, no. 3, p. 15 pages, 2018.

[3] S. Ahsan, Z. Guo, Z. Miao, I. Sotiriou, M. Koutsoupidou, E. Kallos, G. Palikaras, and P. Kosmas, "Design and experimental validation of a multiple-frequency microwave tomography system employing the dbim-twist algorithm," *Sensors*, vol. 18, no. 10, 2018.

[4] M. Azghani, P. Kosmas, and M. Marvasti, "Microwave medical imaging based on sparsity and an iterative method with adaptive thresholding," *IEEE Trans. Med. Imag.*, vol. 34, pp. 357–365, Feb. 2015.

[5] Z. Miao and P. Kosmas, "Microwave breast imaging based on an optimized two-step iterative shrinkage/thresholding method," in *Proc. 2015 9th European Conf. Antennas and Propag. (EuCAP)*, pp. 1–4, May 2015.

[6] Z. Miao and P. Kosmas, "Multiple-frequency DBIM-TwIST algorithm for microwave breast imaging," *IEEE Trans. Antennas Propag.*, vol. 65, pp. 2507–2516, May 2017.

[7] J. D. Shea, P. Kosmas, S. C. Hagness, and B. D. Van Veen, "Three-dimensional microwave imaging of realistic numerical breast phantoms via a multiple-frequency inverse scattering technique," *Medical Physics*, vol. 37, pp. 4210 – 4226, 8 2010.

[8] D. M. Young, "Iterative solution of large linear systems," *Academic Press, New York/ London.*, 1971.

[9] M. Azghani and F. Marvasti, "Iterative methods for random sampling and compressed sensing recovery," in *10th International Conference on Sampling Theory and Applications (SAMPTA 2013)*, 2013.

[10] T. Blumensath and M. E. Davies, "Iterative thresholding for sparse approximations," *J. Fourier analysis Applications*, vol. 14, no. 5-6, pp. 629–654, 2008.

[11] J. M. Bioucas-Dias and M. A. Figueiredo, "A new TwIST: two-step iterative shrinkage/thresholding algorithms for image restoration," *IEEE Transac. Imag. process.*, vol. 16, no. 12, pp. 2992–3004, 2007.

[12] R. Scapaticci *et al.*, "Wavelet-based regularization for robust microwave imaging in medical applications," *IEEE Trans. Biomed. Eng.*, vol. 62, pp. 1195–1202, April 2015.

[13] W. Chew and J. Lin, "A frequency-hopping approach for microwave imaging of large inhomogeneous bodies," *Microwave and Guided Wave Letters, IEEE*, vol. 5, pp. 439–441, Dec 1995.